Submitted to Phys. Rev. B

LBL-1916
Preprint

THE RELATIVE EFFECT OF EXTRA-ATOMIC RELAXATION ON AUGER AND ESCA SHIFTS IN TRANSITION METALS AND SALTS

S. P. Kowalczyk, L. Ley, F. R. McFeely,
R. A. Pollak, and D. A. Shirley

June 1973

Prepared for the U. S. Atomic Energy Commission
under Contract W-7405-ENG-48

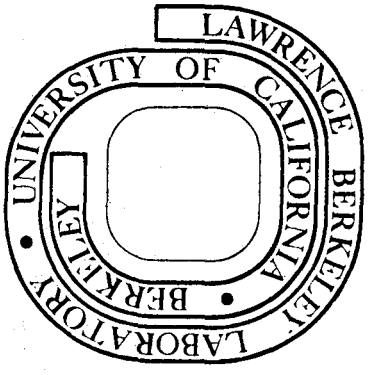

DISCLAIMER

THE RELATIVE EFFECT OF EXTRA-ATOMIC RELAXATION ON AUGER AND ESCA SHIFTS IN TRANSITION METALS AND SALTS*

S. P. Kowalczyk, L. Ley, F. R. McFeely, R. A. Pollak†, and D. A. Shirley

Department of Chemistry and
Lawrence Berkeley Laboratory
University of California
Berkeley, California 94720

June 1973

ABSTRACT

The relation between shifts in Auger energies and shifts in electron binding energies is explored. The prediction of Auger energies in metals from one-hole and two-hole optical energies as well as from electron binding energies in metals is described, with proper accounting for final state coupling, relaxation, and reference energies. A decrease in values of extra-atomic relaxation energies for 3d metals between Ni and Cu, arising from the loss of d-wave screening at the 3d shell closure, was derived for the $L_3M_{23}M_{23}$ Auger transition in which the final state is localized. A similar decrease can be derived from the data on the $L_3M_{45}M_{45}$ transition, suggesting that the 3d hole state may be localized. Shifts in either Auger or ESCA energies between solids have no direct significance when taken alone, but the difference between the two is shown to be equal to the difference in the corresponding extra-atomic relaxation energies. Differential shifts are reported for sodium and its salts and for zinc and its salts. The differential shift between sodium metal and NaF is 8.7 eV, while the Zn to ZnF_2 shift is 5.2 eV, in good agreement with expectations. The Zn(3d) - F(2p) peak in the ZnF_2 spectrum gives clear evidence for crystal-field splitting in the final state.

I. INTRODUCTION

X-ray photoemission (XPS) measurements yield core-electron binding energies; i.e., the energies of processes of the form:

$$M \rightarrow M_i^+ + e^- \quad , \tag{1}$$

where M may be an atom, molecule, or solid, and M_i^+ denotes a final state in which an electron has been removed from orbital i. We denote the binding energy for this process by E(i). Shifts in E(i) are well-known: these are commonly called "ESCA shifts",[1] and are usually regarded as arising from chemical effects, most often oxidation in the ground state (M in this case). We shall denote these shifts as $\delta E(i)$.

Auger processes, which have the form

$$M_j^+ \rightarrow M_{k\ell}^{++} + e^- \quad , \tag{2}$$

also yield electrons of well-defined kinetic energy which often appear as peaks in XPS spectra. These Auger peaks originate from the formation of holes in the core j level through the photoelectric effect, followed by the jkℓ Auger cascade. Thus the Auger kinetic energy, E(jkℓ), is independent of the incident x-ray energy. Shifts in the Auger energy, denoted by $\delta E(jk\ell)$, are also known.

In this paper we shall derive the relationship between $\delta E(jk\ell)$ and the ESCA shifts $\delta E(i)$, with i = j, k, ℓ. To do so we must consider total binding energies and Auger energies rather than just shifts. Both atomic and extra-atomic relaxation energy terms in E(i)[2,3] and E(jkℓ)[4,5,6] are found to play roles in these energies. Our conclusions about the relation of $\delta E(jk\ell)$ and

$\delta E(i)$ are very similar to those reached by Wagner and Biloen,[7] who used a somewhat different approach.

This paper has three main objectives: to analyze the way in which Auger energies can be predicted from binding-energy data, to discuss derived values of extra-atomic relaxation energies in metals, and to present and analyze data showing differences between Auger and ESCA shifts in Na and Zn metals and compounds. A general discussion of the contributions to $E(jk\ell)$ in solids is given in Sec. II. This section has three subsections. In II.A., $E(jk\ell)$ is expressed explicitly in terms of individual one-electron binding energies $E(i)$. The use of optical data on one- and two-hole states is described in II.B. A "d-band shielding" effect in transition metals is discussed in II.C. Experimental results for zinc and sodium salts are presented and discussed in Sec. III. Conclusions are given in Sec. IV.

II. THEORETICAL BACKGROUND

A. Auger Energies and One-Electron Binding Energies

The Auger transition (jkℓ) can be broken up into three steps:

$$M \rightarrow M_j^+ + e^- \tag{3a}$$

$$M \rightarrow M_k^+ + e^- \tag{3b}$$

$$M_k^+ \rightarrow M_{k\ell}^{++} + e^- \quad . \tag{3c}$$

The energies of the last two processes can be subtracted from the first energy to give E(jkℓ). The energies of steps (a) and (b) are simple one-electron binding energies E(j) and E(k), which can be used directly. The binding energy in step (c) must be modified, however, to account for the effects on E(ℓ) of electronic relaxation in step (b) and of two-hole coupling in the final state. As discussed earlier,[4-6] these two effects yield an energy $E(\ell)^*$ for step c of the form

$$E(\ell)^* = E(\ell) + \mathcal{F}(k\ell;X) - R(k\ell) \quad , \tag{4}$$

in which $\mathcal{F}(k\ell;X)$ is the interaction energy between the k- and ℓ-holes in the final state X and R(kℓ) is the relaxation energy. The Auger energy is then given as

$$\begin{aligned} E(jk\ell;X) &= E(j) - E(k) - E(\ell)^* \\ &= E(j) - E(k) - E(\ell) - \mathcal{F}(k\ell;X) + R(k\ell) \quad . \end{aligned} \tag{5}$$

We note at this point that the choice of reference energy level for E(jkℓ) and E(i) has no effect on the validity of Eq. (5); if a consistent energy (e.g.,

the Fermi energy) is chosen for both the Auger and binding energies, then any error of variation in this reference energy will cancel out on the two sides of Eq. (5).

The $\mathcal{F}(k\ell;X)$ term is readily calculable[5,6] using standard multiplet coupling theory and tabulated Slater integrals.[8] The relaxation term, $R(k\ell)$, can be estimated rather well in some cases;[4-6] in others the estimation of R is less straightforward. To discuss this problem, we first write R as the sum of an atomic relaxation energy R_a, arising mainly from the collapse of other electronic orbitals of the host atom toward the k hole in step (3b), plus an extra-atomic relaxation[6] term R_e,

$$R = R_a + R_e \quad . \tag{6}$$

Let us consider R_a first. There are two important contributions to R_a: outer-shell relaxation and intra-shell relaxation.[4,5] Their relative magnitudes vary with the relative numbers of electrons outside the "final" shell (e.g., the L shell in KLL Auger processes) and in that shell. Thus for a KLL transition in a heavy element it is quite satisfactory to consider only outer-shell relaxation and the "equivalent core" method gives good results.[5] For neon, on the other hand, intrashell relaxation alone is present. In fact for the cases discussed below (the Na KLL and Zn LMM transitions) the intrashell effect is dominant. As was pointed out earlier,[6] the intrashell relaxation energy can be estimated as twice the dynamic intrashell relaxation energy E_R(intrashell),

$$R_a(\text{intrashell}) \cong 2E_R(\text{intrashell}) \quad . \tag{7}$$

Calculations of E_R are available from optimized Hartree-Fock-Slater calculations on hole states.[9] We note that these values of E_R are useful for our purposes irrespective of whether the hole-state calculations predict binding energies accurately, because the latter question is affected by correlation effects which are omitted in the Hartree-Fock formalism.

Extra-atomic relaxation R_e occurs through a flow of electronic charge toward the host atom during step 3b. It has the effect of making the initial-state environment in step 3c more repulsive and of lowering the binding energy $E(\ell)^*$. R_e is expected to be largest for metals, in which electrons from the valence band can screen the k-hole charge locally, by being drawn down out of the conduction band into a localized state c drawn down out of the conduction band.[3,6] In the limit of completely local screening the screening charge can be regarded as occupying the first unfilled atomic orbital above the Fermi energy E_F, and R_e is then given by the two-electron interaction between this orbital and the ℓ orbital,

$$R_e \cong \mathcal{F}(\ell,c)_k \equiv F^o(\ell,c) + \cdots \quad , \tag{8}$$

where c denotes the conduction-band state, k indicates that this term arises because of the k hole, and the terms beyond F^o (which is always by far the dominant term) are appropriate Slater (Coulomb and exchange) integrals. Thus the Auger energy in a metal is given by an expression of the form

$$E(jk\ell;X) = E(j) - E(k) - E(\ell) - \mathcal{F}(k\ell;X) + 2E_R(\ell) + \mathcal{F}(\ell,c)_k \quad . \tag{9}$$

Again we note that all four quantities $E(jk\ell)$, $E(i)$ $(i = j, k, \ell)$ must be taken relative to the same reference energy.

In an application to the $L_3M_{45}M_{45}$ Auger spectra of Cu and Zn, Eq. (9) gave very good results.[6] The predicted kinetic energies relative to E_F of the

^1D lines were 921.1 eV in Cu and 993.2 eV in Zn, while experiment gave 918.0(2) and 991.8(2), respectively. This good agreement provided strong evidence for localized screening, because extra-atomic relaxation terms $\mathcal{F}(\ell,c)$ of 9.6 (Cu) and 11.0 eV (Zn) were involved in the theoretical estimates. We were then led to inquire how effectively screening by extra-atomic relaxation can occur in non-metals. If the R_e term is smaller in salts, for example, then one would expect significant shifts in the Auger line to lower kinetic energies from metals to salts. Such an Auger shift would arise not from chemical shifts *per se*, which would affect the E(i) terms, but rather from the R term. Of course Auger shifts between two substances have meaning only if the lines are referred to meaningful reference energies. The Fermi energy does not qualify in this case, but the vacuum level does, for the same reason that holds for ESCA shifts. In the following discussion we shall show that the core level photoemission lines can serve as a reference, and we shall also develop methods for isolating the extra-atomic relaxation energy by using optical data.

B. The Use of Optical Data on Free Atoms

As an alternative to using Eq. (9) to predict Auger energies in metals, we can derive Auger energies for free atoms, $E^A(jk\ell)$, from optical data,[10] usually in combination with x-ray energies[11] and/or calculated atomic binding energies.[9,12] First let us estimate $E^A(jk\ell)$ from free-atom one-electron binding energies $E^A(i)$. By going through a three-step process similar to Eq. (3a,b,c) for free atoms, it is easy to derive the relation

$$E^A(jk\ell;X) = E^A(j) - E^A(k) - E^A(\ell) - \mathcal{F}(k\ell;X) + 2E_R(\ell) \quad , \qquad (10)$$

which differs in form from Eq. (9) only in having no extra-atomic relaxation term. To apply this result to the ($L_3M_{45}M_{45}$; ^1D) Auger transition in atomic copper, for example, we can use the data collected in Table I to find

$$E^A(L_3M_{45}M_{45};\ ^1D)_{Cu} = 903.9 \text{ eV} \quad ,$$

for atomic copper.

Returning to our general notation, we note that the Auger process, like photoemission, is one in which one electron is lost. Thus the Auger energy in a solid could be compared directly to that in an atom only if the former were referred to the vacuum level. If it is referred to the Fermi level, $E^F(jk\ell)$, a correction for the work function ϕ must be made. The two Auger energies also differ by the total Auger extra-atomic relaxation, which we shall denote by $R_e(TA)$. Thus

$$E^F(jk\ell) = E^A(jk\ell) + e\phi + R_e(TA) \quad . \tag{11}$$

For the copper ($L_3M_{45}M_{45}$; ^1D) case we have $E^F = 918.0$, while $\phi = 4.5$ eV.[13] Combining these with Eqs. (10) and (11), we find

$$R_e(TA) = 9.6 \text{ eV} \quad .$$

By coincidence this has the same value as the theoretical estimate of $\mathcal{F}(\ell,c)_k$ for copper, mentioned above. In fact $R_e(TA)$ should be about 50% larger than $\mathcal{F}(\ell,c)_k$. To understand this we note that atomic binding energies were used in Eq. (11), while Eq. (9) was based on binding energies in the metals. We may relate the two, and also derive a method for estimating $R_e(TA)$ theoretically, by going once again through a three-step sequence as in Eq. (3), but this time relating the energy of each step in the metal to that in the free atom. This gives

$$E^F(j) = E^A(j) - e\phi - \tfrac{1}{2} \mathcal{F}(jc) \qquad (12a)$$

$$E^F(k) = E^A(k) - e\phi - \tfrac{1}{2} \mathcal{F}(kc) \qquad (12b)$$

$$E^F(\ell)^* = E^A(\ell)^* - e\phi - \mathcal{F}(\ell c)_k - \tfrac{1}{2} \quad (\ell c) \quad . \qquad (12c)$$

Here $\frac{1}{2} \mathcal{F}(ic)$ is the amount by which the binding energy of the i^{th} orbital is lowered in the metal through dynamic extra-atomic relaxation[5] of the conduction band. Combining Eqs. (12) to form Auger energies, we find

$$E^F(jk\ell) = E^A(jk\ell) + e\phi + \mathcal{F}(\ell c)_k + \tfrac{1}{2} [\mathcal{F}(\ell c) + \mathcal{F}(kc) - \mathcal{F}(jc)] \quad . \qquad (13)$$

Thus the total Auger extra-atomic relaxation is given by

$$R_e(TA) = \mathcal{F}(\ell c)_k + \tfrac{1}{2} [\mathcal{F}(\ell c) + \mathcal{F}(kc) - \mathcal{F}(jc)] \quad , \qquad (14)$$

from Eqs. (11) and (13). Since $\mathcal{F}(\ell c)_k$ and the three quantities $\mathcal{F}(ic)$ ($i = j, k, \ell$) are all of approximately the same size (as will be shown below for the case of copper, $R_e(TA)$ is about 1.5 times as large as $\mathcal{F}(\ell c)_k$.

Specializing now to the copper ($L_3M_{45}M_{45}$; ^1D) Auger transition, we substitute L_3 for j, etc., in Eq. (14), expand the $\mathcal{F}(ic)$ in terms of Slater integrals, invoke the equivalent-cores approximation, and use Mann's values[8] for these integrals. In this case $k = \ell$; thus $\mathcal{F}(\ell c)_k = \mathcal{F}(kc)$, but $\mathcal{F}(kc) \neq \mathcal{F}(\ell c)$ since in $\mathcal{F}(kc)$ a conduction electron (which we assume to be 4s) is screening a single hole, so that Slater integrals in zinc are appropriate, whereas in $\mathcal{F}(\ell c)$ the conduction electron (which we take as 4p) is screening a second hole and gallium is the equivalent core. Thus

$$\mathcal{F}(jc) \cong [F^{o}(2p,4s) - \tfrac{1}{6} G^{1}(2p,4s)]_{Zn} = 11.7 \text{ eV}$$

$$\mathcal{F}(kc) = \mathcal{F}(\ell c)_{k} \cong [F^{o}(3d,4s) - \tfrac{1}{10} G^{2}(3d,4s)]_{Zn} = 11.0 \text{ eV}$$

$$\mathcal{F}(\ell c) \cong [F^{o}(3d,4p) - \tfrac{1}{15} G^{1}(3d,4p) - \tfrac{3}{70} G^{3}(3d,4p)]_{Ga} = 9.6 \text{ eV} \quad .$$

Thus from Eq. (14), we have

$$R_{e}(TA, CuL_{3}M_{45}M_{45}; {}^{1}D) = 15.5 \text{ eV} \quad .$$

This estimate exceeds the "experimental" value of 9.6 eV given above, presumably because the screening charge is not as localized as this approach assumes. This estimate (15.5 eV) together with $\phi = 4.5$ eV and the free-atom estimate for $E^{A}(L_{3}M_{45}M_{45}; {}^{1}D)$, leads to an estimated Auger energy for the ^{1}D line in metallic copper of

$$E^{F}(L_{3}M_{45}M_{45}; {}^{1}D) \cong 923.9 \text{ eV} \quad ,$$

or 6 eV larger than the experimental value of 918 eV.

Another approach that also employs optical data is based on the use of the one- and two-hole states in free atoms that correspond to the initial and final states in the Auger transition. Denoting these by $E^{A}(j)$ and $E^{A}(k\ell)$, we have $E^{A}(jk\ell) = E^{A}(j) - E^{A}(k\ell)$, and this quantity can go directly into Eq. (11), giving

$$E^{F}(jk\ell) = E^{A}(j) - E^{A}(k\ell) + e\phi + R_{e}(TA) \quad . \qquad (15)$$

In the copper example above $E^A(j)$ is the $Cu(\overline{2p}_{3/2})^+$ state at 940.1 eV (Table I), while the appropriate ^1D final state lies at the weighted mean energy of the $3d^8(^1D)4s;\ ^2D_{3/2}$ and $3d^8(^1D)4s;\ ^2D_{5/2}$ states in Cu III; i.e., at 37.72 eV above the ground state of Cu I. Thus we estimate

$$E^A(L_3M_{45}M_{45};\ ^1D) = 902.4 \text{ eV} \quad ,$$

using this approach. From Eq.(15), the experimental value $E^F = 918.0$ eV, and $e\phi = 4.5$, eV, we find

$$R_e(TA) = 11.1 \text{ eV} \quad ,$$

in better agreement with the theoretical estimate of 15.5 eV. This "two-hole" estimate of $R_e(TA)$ is preferred because it uses more optical data and fewer assumptions than does the "one hole" method based on Eq. (10).

Careful bookeeping is required at several points in discussing extra-atomic relaxation energies for Auger transitions in metals. Only two simple concepts are involved, however. First, as a charge q is removed from an atom, a screening charge q moves in, reducing the binding energy by the dynamic relaxation energy $R_e = \frac{1}{2} q^2/r_{eff}$ classically, where r_{eff} is an effective screening radius. In quantum-mechanical language, n electrons are removed, $q = n|e|$, and $R_e = \frac{1}{2} n^2 \mathcal{F}$, where $\mathcal{F}$ is a linear combination of Slater integrals in the limit of localized screening. Second, if the Auger energy is estimated by summing over one-electron binding energies, then an additional static relaxation term must be added (e.g., in Eq. (3c)). This amounts to $R_e = \mathcal{F}$, or e^2/r_{eff} classically.

When one-electron binding energies in metals $E^F(i)$ are used to estimate $E^F(jk\ell)$, as in Eq. (9), the dynamic screening effects are included in the E(i). Thus only the static term remains, and $R_e = \mathcal{F}$.

If one-electron atomic binding energies $E^A(i)$ are used, each must be reduced by $\frac{1}{2}\mathcal{F}$ to account for dynamic extra-atomic relaxation in the metal. Because these binding energies appear in the combination E(j) - E(k) - E(ℓ), two of the $\frac{1}{2}\mathcal{F}$ terms will cancel, leaving a net dynamic term $\frac{1}{2}\mathcal{F}$ to be added to the static term $\mathcal{F}$, giving the total Auger extra-atomic relaxation energy $R_e(TA) = \frac{3}{2}\mathcal{F}$.

If one- and two-hole atomic states (j) and (kℓ) are used, there is no static term. The dynamic terms by which E(j) and E(kℓ) must be corrected are $\frac{1}{2}\mathcal{F}$ and $2\mathcal{F}$, respectively, for n = 1, and 2. The net correction is therefore $\frac{3}{2}\mathcal{F}$, as above.

In summary, we have explored three ways to derive the energy associated with extra-atomic relaxation of Auger transitions in solids. They are based on comparison of experimental Auger energies with:

1. One-electron binding energies in solids[6] (Eq. (9); this gives $\mathcal{F}(\ell,c)$).
2. One-electron binding energies in atoms (Eq. (11); giving $R_e(TA)$).
3. Initial and final Auger states in atoms (Eq. (15); giving $R_e(TA)$).

Both $\mathcal{F}(\ell,c)$ and $R_e(TA)$ can be estimated theoretically on the equivalent cores model, as described previously[6] and above. Results for the $(L_3M_{45}M_{45}; {}^1D)$ transition in Cu, derived above, are collected in Table II.

These results further substantiate the earlier observation of extra-atomic relaxation accompanying Auger transitions in metals[6] as well as showing

how atomic optical data can be used to isolate $R_e(TA)$. Since the 3d hole states now appear to be essentially localized and the screening at least semi-localized in copper, it would be valuable to determine the extent to which this is true in the transition metals, which have open 3d shells. We address this question below.

C. Hole-State Localization and d-Wave Screening in Transition Metals

In a recent analysis of the effect of extra-atomic relaxation on the binding energies of core electrons in transition metals, striking evidence was found for d-wave screening through Ni and s,p wave screening for Cu and Zn.[3] The quantity $\delta E(i) = E^A(i) - E^F(i) - e\phi$ which should be $\frac{1}{2}\mathcal{F}(i,c)$ according to Eq. (12b), rises to 12-13 eV for Co and Ni, then drops to 3-4 eV in Cu and Zn. This is expected because the d-band fills between Ni and Cu. The experimental $\delta E(i)$ were only about $\frac{2}{3}$ as large for the transition metals as the theoretical estimates of $\frac{1}{2}\mathcal{F}(i,c)$ based on atomic integrals, suggesting the screening is not completely localized (or to be more precise, that the conduction-band d-state doing the screening is less localized than an atomic 3d function). In this case there was no doubt that the hole state was localized, because it was in the n = 2 shell. The results are reproduced, for comparison purposes, in Fig. 1a.

Let us next consider an Auger transition in which the final state is certainly localized; the $L_3M_{23}M_{23}$ transition. Data are incomplete and of variable quality for this transition, but we have derived tentative values of $R_e(TA)$ from available data, using the relation

$$R_e(TA) \cong E^F(L_3M_{23}M_{23}) - E^A(L_3) + 2E^A(M_{23}) + F^o(3p,3p) - e\phi - 2E_R(3p) \quad , (16)$$

which follows from Eqs. (10) and (11), if final-state multiplet splitting is neglected and $\mathcal{F}(k\ell;X)$ is approximated as $F^{o}(k\ell)$. Auger energies were taken from the compilation of Haynes.[14] Even at this level of approximation several of the data needed in Eq. (16) are not very reliably known, and we have serious reservations about the accuracy with which we have estimated $R_e(TA)$. The values of the parameters that we used are given in Table III. Also listed are theoretical estimates of $R_e(TA)$ based on the approach described above in Sec. II.B. Both $R_e(TA)_{expt}$ and $R_e(TA)_{theo}$ are plotted in Fig. 1b. The transition from d-wave to s, p-wave screening between Ni and Cu appears to be present here as well. In this case the magnitude of the d-wave screening is also about $\frac{2}{3}$ of the "localized" estimates, while for Cu and Zn the two agree very well. At this level of detail, however, further refinements in the data and/or analysis may modify this conclusion.

Having established above that a "shell effect" in $R_e(TA)$ exists, for an Auger transition with a localized final state, at the 3d-shell closure between Ni and Cu, we can test whether the $(L_3M_{45}M_{45})$ Auger energies are consistent with a localized final state. The relevant equation in this case is

$$R_e(TA) \cong E^F(L_3M_{45}M_{45}) - E^A(L_3) - e\phi + 2E^A(M_{23}) + F^o(3d,3d) - 2E_R(3d) \quad . \quad (17)$$

Proceeding as for the $(L_3M_{23}M_{23})$ case, we have derived values of $R_e(TA)$ from the data in Table IV, and plotted them in Fig. 1c. The results are certainly <u>consistent</u> with localized 3d hole states and a shell effect between Ni and Cu. We are, however, reluctant to infer that the Auger final states are definitely localized, because we have in a sense assumed this in the structure of Eq. (17). If the 3d holes were delocalized the last three terms in Eq. (17) would all be

smaller, and R_e(TA) would be smaller than Eq. (17) implies. Thus it could certainly be argued that our analysis tends to exaggerate the localized nature of the hole states by using terms such as $F^o(3d,3d)$ in the estimates of R_e(TA). It seems quite clear that the Cu and Zn Auger transitions involve localized 3d hole states: the Auger peaks in Cu are narrower than the 3d band and the Auger peak structure in both Cu and Zn follows multiplet splitting predictions quite closely.[6] For the 3d transition metals, however, further work is needed before the Auger hole states can be taken as localized.

Proceeding to the fifth-row elements, there are as yet too few data available to discuss the systematic variation of R_e(TA) with Z. It is, however, evident that localized hole states are present in the $M_{45}N_{45}N_{45}$ spectrum of silver, as reported recently by C. J. Powell.[15] We have carried out a rough analysis of the available Auger data on this transition in the 4d series Ru, Rh, Pd, and Ag, to derive $R_e(\cong \frac{2}{3} R_e(\text{TA}))$ for these elements. The relation

$$R_e \cong E^F(M_5N_{45}N_{45}) - E^F(M_5) + 2E^F(N_{45}) + F^o(4d,4d) - 2E_R \quad , \qquad (18)$$

which follows from Eq. (9) with $R_e \equiv \mathcal{F}(\ell,c)$, was used. Table V lists the numerical values of the energy parameters. Several of these energies have been determined experimentally by XPS studies in our laboratory. There is no evidence for an abrupt decrease in R_e from Pd to Ag due to closure of the 4d shell, in contrast to the result for Ni and Cu. There is apparently a large decrease from Ru to Pd and Ag, however. This would be consistent with the atomic ground states, because Pd has a ground-state configuration $4d^{10}$ (whereas Ni is $3d^8 4s^2$); thus R_e(Pd) might be expected to arise mainly from s-wave screening if its d-band were nearly full and hence be smaller than R_e(Ru)

or R_e(Rh). We are, however, again reluctant to draw a firm conclusion that this is in fact the case until more complete data are available and a more detailed analysis can be made.

For both the 3d- and 4d-series Auger spectra we have had to draw only tentative conclusions. Nevertheless there is enough evidence for the effect of shell closure on R_e in each case to justify further work. It appears quite possible that with further analysis of R_e values we may be able to determine the extent of localization of d-hole states in transition metals.

III. EXTRA-ATOMIC RELAXATION AND AUGER ENERGIES IN ZINC AND SODIUM SALTS

To assess the extent to which variations in extra-atomic relaxation energy can affect Auger energies, we have selected the (KLL; ^1D) transition in sodium and the ($L_3M_{45}M_{45}$; ^3P, ^1G, ^1D) peak in zinc as examples that are sufficiently well-characterized for this study. These two cases are discussed separately below.

The experimental measurements were done in a Hewlett-Packard HP 5950A ESCA Spectrometer. The sodium metal (KLL; ^1D) Auger energy, together with the 1s and 2p binding energies, have been reported earlier.[16] They are given in Table VI for convenience. Also listed are E^F(KLL; ^1D), E^F(K), and $E^F(L_{23})$ for sodium oxide, obtained from a sodium metal sample after it was slightly oxidized. The XPS spectrum of this sample agreed well with that of Fahlman, et al.,[17] who prepared their sample in a similar way. We have also carried out XPS studies on single crystals of NaF and NaI, and Table VI lists the relevant binding energies and Auger energies. In these cases the reference energy is the top of the valence band in each case. In the NaF work we did not obtain a satisfactory value for E(1s) experimentally, and we assumed that E(1s) - E(2p) = 1042 eV, the value for NaI (this estimate should be accurate to 1 eV or better since both the 1s and 2p states are core levels. Empirically, the 1s - 2p splitting is nearly constant even from the metal to the salts, as the data in Table VI show).

To analyze the sodium data we can use all three methods discussed in Sec. II.B, and they all show quite good agreement. We shall present here a comparison of the atomic Auger energies E^A(KLL; ^1D) as calculated from data on one- and two-hole optical states, to test this approach. The two-hole calculation will then be taken as providing an empirical value of the

combination of terms $-\mathcal{F}(k\ell;X) + 2E_R(\ell)$ in Eq. (10). This quantity will be used to derive extra-atomic relaxation energies in the solids.

For atomic sodium, Eq. (10) becomes

$$E^A(KLL;\ ^1D) = E^A(K) - 2E^A(L_{23}) - \mathcal{F}(2p,2p;\ ^1D) + 2E_R(2p) \quad . \qquad (19)$$

We have used the values E(K) = 1079.1 eV, obtained from optical[10] and x-ray[11] data, and also theoretically,[12] $E(L_{23})$ = 38.02 eV,[10] E_R = 4.7 eV,[9] and

$$\mathcal{F}(2p,2p;\ ^1D) = F^o(2p,2p) - \frac{2}{25}F^2(2p,2p) - \frac{1}{4}\zeta + \{(\frac{3}{25}F^2(2p,2p) + \frac{1}{4}\zeta)^2 + \frac{1}{2}\zeta^2\}^{1/2} \quad ,$$

as given by Asaad and Burhop.[18] Using Mann's values for the Slater integrals[8] and optical data for the spin-orbit coupling constant ζ,[10] we calculated a numerical value $\mathcal{F}(2p,2p;\ ^1D)$ = 32.17 eV. Thus

$$E^A(KLL;\ ^1D) = 980.3 \text{ eV} \quad ,$$

as estimated from optical data on one-hole states.

The mean energy of the $1s^2 2s^2 2p^4(^1D)3s$ state in Na III lies 101.92 eV above the ground state of Na I.[10] We can estimate the Auger energy as

$$E^A(KLL;\ ^1D) = E^A(K) - E^A(1s^2 2s^2 2p^4(^1D)3s) = 977.2 \text{ eV} \quad .$$

The discrepancy of 3.1 eV between this result and the above one-hole state estimate is an indication of the accuracy of the latter (note the similar discrepancy of 1.5 eV, in the same direction, for Cu in Sec. II.B). The two-hole state result is preferred because it uses empirical data exclusively. Since it will be necessary to use one-hole energies (Eq. (9)) for analyzing

Auger energies in the solids, we can combine the above result (977.2 eV) with Eq. (19), E(K) = 1079.1 eV, and $E(L_{23})$ = 38.02 eV to obtain a reliable empirical estimate of

$$-\mathcal{F}(2p,2p;\ ^1D) + 2E_R(2p) = -25.86 \text{ eV} \quad ,$$

for later use.

The above values of $E^A(KLL;\ ^1D)$ can be compared with experiment. Sevier[19] quoted experimental studies of the Na(KLL) Auger spectrum on Na vapor, in which the measured energies were 13 - 15 eV lower than those reported by Fahlman, et al.,[17] for the oxide. This would correspond to (990 - 13 to 15) = 975 - 977 eV for the ^1D line, in good agreement with the above value.

The extra-atomic relaxation energies in the solids in Table VI were obtained from the relation

$$R_e = E^F(KLL;\ ^1D) - E^F(1s) + 2E^F(2p) + 25.86 \text{ eV} \quad , \qquad (20)$$

which follows from Eq. (9) and the discussion above, with $\mathcal{F}(\ell,c) = R_e$. The largest value of R_e, 9.2 eV, is found in the metal. It agrees very well with the value

$$R_e(2p,3s) \cong [F^o(2p,3s) - \tfrac{1}{2} G^1(2p,3s)]_{Mg} = 9.7 \text{ eV} \quad ,$$

estimated on the equivalent-cores model.[16] In the salts, as Wagner and Biloen have pointed out,[7] screening charges remain on neighboring ions, and R_e should be smaller. This expectation is borne out very nicely in Table VI. It is pleasing (although perhaps fortuitous) that the three salts have R_e values ordered according to their anion electronegativities.

It is not always feasible to calculate R_e in solids from Auger and binding-energy data in the way described above. Unfortunately, neither binding energy shifts nor Auger shifts alone are very meaningful, because there is no reliable reference energy if these energies are compared from one solid to another. A meaningful energy shift does exist, however; it is the shift in the difference energy between the binding energy of one of the final state holes and the apparent binding energy in the XPS spectrum of the Auger line, $E_B(jk\ell) = h\nu - E(jk\ell)$, where $h\nu$ is the photon energy. Substituting this relation into Eq. (9), with $\mathcal{F}(\ell,c) = R_e$, we have

$$h\nu - E_B(jk\ell) = E(j) - E(k) - E(\ell) - \mathcal{F} + 2E_R + R_e \quad ,$$

or

$$E(\ell) - E_B(jk\ell) = E(j) - E(k) - h\nu - \mathcal{F} + 2E_R + R_e \quad .$$

Now $E(j) - E(k)$ is the energy of an x-ray connecting two core states. It shifts very little with changes of environment. The combination of terms $-\mathcal{F} + 2E_R$ is an atomic property which should also be constant from one material to another, and of course $h\nu$ doesn't vary. Thus to a very good approximation,

$$\Delta[E(\ell) - E_B(jk\ell)] = \Delta R_e \quad . \tag{21}$$

That this relationship holds well for Na is shown by comparing the last two columns of Table VI. It is useful because $E(\ell)$ and $E_B(jk\ell)$ have a common reference energy; therefore the reference energy need not be known to

determine ΔR_e. The relative shifts in $E_B(KLL; {}^1D)$ and $E(2p)$ for Na, as well as the constancy of $E(1s) - E(2p)$, is illustrated in Fig. 2.

The $L_3M_{45}M_{45}$ transition in zinc was studied in the metal,[6] in a single crystal of ZnO, and in several ZnF_2 samples. The Zn Auger spectrum was reported earlier.[6] The ZnF_2 spectrum is shown in Fig. 3. The ZnF_2 work was done on single crystals, but sample charging shifted the lines by several electron volts, necessitating wide scans in which at least two lines were intercompared, with consequent loss of accuracy. One experiment was also carried out on a single crystal sample at Hewlett-Packard, Inc., in Palo Alto, in which charging was neutralized by an electron flood gun. The ZnF_2 energies, which are listed in Table VII, are values obtained by combining the average of the splittings in a total of four experiments with the Zn(3d) binding energy from the flood-gun experiment.

The equation

$$R_e(Zn) = E^F(L_3M_{45}M_{45}) - E^F(2p_{3/2}) + 2E^F(3d) + \mathcal{F}(3d,3d; {}^1D) - 2E_R \quad , \quad (22)$$

can be used to obtain R_e for the ^1D peak in zinc. It was obtained from Eq. (9) with $\mathcal{F}(\ell,c) = R_e(Zn)$. There are no suitable two-hole optical data available for zinc, to our knowledge. The last two terms in Eq. (22) were therefore taken from Ref. 6, which gave $\mathcal{F}(3d,3d; {}^1D) - 2E_R = 16.6$ eV. Again the extra-atomic relaxation term R_e is larger in the metal than in the oxide or fluoride, as expected. The apparent binding energy shift $E(3d) - E_B({}^1D)$ increases by 5.2 eV from ZnF_2 to Zn metal, in reasonable agreement with the 4.0 eV increase in R_e. Thus the Auger shifts in zinc and zinc compounds behave as expected, in agreement with the sodium results.

Returning now to the relation between Auger shifts $\delta E(jk\ell;X)$ ESCA shifts $\delta E(i)$, we can derive from Eq. (5) the variation of these shifts between two environments as

$$\delta E(jk\ell;X) = \delta E(j) - \delta E(k) - \delta E(\ell) + \delta R(k\ell) \quad . \tag{23}$$

We have assumed here that $\mathcal{F}(k\ell;X)$ does not vary with environment. Equation (23) displays explicitly the important role played by changes in relaxation energy $\delta R(k\ell)$ relative to ESCA shifts. Applying this relation to the $(KLL;\ ^1D)$ transition in sodium, and using the data in Table VI, we have for the shifts from metal to oxide:

$$\delta E(KLL;\ ^1D) = \delta E(1s) - 2\delta E(2p) + \delta R$$

$$-7.4 \text{ eV} = -1.3 \text{ eV} + \delta R$$

$$-6.1 \text{ eV} = \delta R \quad .$$

Thus the shift in relaxation energy (-6.1 eV) is much more important than the net binding-energy shift (-1.3 eV) in determining the Auger shift of -7.4 eV in this case. Clearly this is not always true (e.g., the ESCA shifts are more important in the NaI versus oxide shift), but it would be grossly inaccurate to omit the δR term in Eq. (23).

In analyzing the ZnF_2 spectra we found a peculiar peak shape in the Zn 3d - F 2p region which cannot be interpreted in terms of two simple peaks: we attribute this peak shape to crystal-field splitting in the final state. Wertheim, et al.[20] have interpreted several XPS spectra of transition-metal compounds in terms of final-state crystal-field splitting, and Novakov has observed these effects in cobalt salts.[21] In the case at hand (ZnF_2) the evidence for crystal-field splitting is especially compelling, both because the satellite structure on the main 3d peak falls at lower binding energies (thereby precluding alternate interpretations in terms of energy losses or shake-up structure) and because independent cross-section and energy arguments can be invoked. The spectrum is shown in Fig. 4. We list below the arguments for interpreting the Zn 3d - F 2p structure in terms of crystal-field splitting (Interpretation A) instead of just a Zn 3d peak plus a F 2p peak (Interpretation B).

1. The spectrum cannot be fitted with only two peaks: the low-E_B pedestal is too broad.
2. The area under the pedestal (a_p) is too large to be attributable to the F 2p shell alone. The area ratio of the F(2s) peak (not shown) to a_p is 1.3, while the ratio obtained from three other fluorides that we have recently studied are F(2s)/F(2p) = 4.9 (LiF), 4.7 (KF), and 4.1 (MnF_2).
3. The F(2s) - F(2p) spacing in the above compounds is 20.9(2) eV, while the pedestal in Fig. 4 extends to $\sim$ 23 eV from the 2s peak.
4. If only the main peak in Fig. 4 were taken as containing all the 3d strength (Interpretation B), the Zn(2p)/Zn(3d) ratio would be 3.3, whereas this ratio is only 2.5 in Zn metal.

5. Finally, the $Zn(2p_{3/2})$ - Zn(3d) spacing (Table VII) would be anomalously low, by 1 eV, if the 3d strength all lay in the main peak. The 3d position given in Table VII was based on Interpretation A.

While these arguments appear to establish the existence of final-state crystal-field splitting unambiguously, the exact nature of the final state levels is elusive. The D_{4h} symmetry of ZnF_2 should split the single-hole $3d^9$ final states beyond the t_{2g} and e_g levels expected in an octahedral field. Any estimate of the extent of this distortion would be rather speculative, however. The initial-state geometry is not applicable, and the effective crystal field in the final state is hard to assess, because the speed of the photoemission process implies relaxation of the F(2p) electrons toward the hole state but essentially no nuclear motion. The magnitude of the splitting (4 eV or 3×10^4 cm^{-1} total) is unusually large for a transition-metal compound. We note, however, that: (1) even if relaxation were complete, the total splitting should be comparable to optical values of 10 Dq from tripositive ions; i.e. 2×10^4 cm^{-1} rather than $\sim 10^4$ cm^{-1}; (2) the final-state crystal-field strength should be further increased during the effective sampling time of the XPS experiment ($\sim 10^{-15}$ sec) by the fact that ligand electrons can relax toward the hole state in this time interval while ligand nuclei cannot. This will enhance the effective negative charge on the ligands. Finally, then, we are unable to state whether the 3d structure should be analyzed, after the F 2p intensity is subtracted out, as two peaks (t_{2g} and e_g) with intensity ratio $\sim$ 3:2, or as three peaks (because of further splitting in the tetragonal field) with intensities 3:1:1. The peak structure shown in Fig. 4 can be analyzed into

peaks of relative intensities $\sim$ 3.5:1. This may denote extreme tetragonal distortion, which would split one d-level out and leave the other four rather close together,[22] giving a 4:1 intensity ratio. Since the spectrum does not allow us to decide conclusively among the various possibilities, we simply note here that there is crystal-field splitting present in the final state and report the mean binding energy as E(3d) in Table VII.

IV. CONCLUSIONS

The principal conclusions from this work are listed below:

1. Auger energies in metals can be predicted from free-atom optical data (in two ways) or from solid-state data, provided that proper account is taken of final-state coupling and extra-atomic relaxation energies. Predicted values agree well among themselves and with experiment.
2. Extra-atomic relaxation accounts for energy differences of 10 eV or more between free-atom and metal Auger energies.
3. Auger energies in 3d transition metals are consistent with an abrupt drop in extra-atomic relaxation energy between Ni and Cu, which is consistent with expected cessation of d-wave screening of localized 3d hole states.
4. Relative shifts of core-level binding energies and Auger energies of 8.7 eV (Na vs NaF) and 5.2 eV (Zn vs ZnF_2) were observed. These were attributed mainly to differences in extra-atomic relaxation energies, which were analyzed to be 9.4 eV and 4.0 eV, respectively.
5. Thus while shifts in neither core-level binding energy nor Auger energy from one solid to another have precise meaning, relative shifts can be interpreted readily.

ACKNOWLEDGMENTS

We gratefully acknowledge gifts of ZnO single crystal from Prof. G. A. Somorjai, ZnF_2 single crystal from Dr. R. Feigelson, and NaF and NaI from Dr. N. M. Edelstein.

FOOTNOTES AND REFERENCES

*Work performed under the auspices of the U. S. Atomic Energy Commission.

†Present Address: IBM, T. J. Watson Research Center, Yorktown Heights, N. Y. 10598.

1. For a recent discussion of ESCA shifts, see D. A. Shirley, Advances in Chemical Physics 23, 85 (1973).

2. D. A. Shirley, Chem. Phys. Letters 16, 220 (1972).

3. L. Ley, S. P. Kowalczyk, F. R. McFeely, R. A. Pollak, and D. A. Shirley, Phys. Rev. B, to be published.

4. D. A. Shirley, Chem. Phys. Letters 17, 312 (1972).

5. D. A. Shirley, Phys. Rev. A7, 1520 (1973).

6. S. P. Kowalczyk, R. A. Pollak, F. R. McFeely, L. Ley, and D. A. Shirley, Phys. Rev. B, to be published, August, 1973.

7. C. D. Wagner and P. Biloen, Surface Science 35, 82 (1973).

8. J. B. Mann, "Atomic Structure Calculations I. Hartree Fock Energy Results for the Elements Hydrogen to Lawrencium", LA-3690, TID 4500 (1967).

9. U. Gelius and K. Siegbahn, "ESCA Studies of the Molecular Core and Valence Levels in the Gas Phase", UUIP-794 (unpublished) (September, 1972).

10. C. E. Moore, "Atomic Energy Levels" (U. S. Dept. of Commerce, NBS Circular No. 467) Vol. 1 (1949); Vol. 2 (1952); Vol. 3 (1958).

11. J. A. Bearden, Rev. Mod. Phys. 39, 78 (1967).

12. K. Siegbahn, C. Nordling, A. Fahlman, R. Nordberg, K. Hamrin, J. Hedman, G. Johansson, T. Bergmark, S.-E. Karlsson, I. Lindgren, and B. J. Lindberg, ESCA - Atomic, Molecular and Solid State Structure by Means of Electron Spectroscopy, Nova Acta Regiae Soc. Sci. Upsaliensis Ser. IV, Vol. 20 (1967).

13. D. E. Eastman, Phys. Rev. B2, 1 (1970).

14. S. K. Haynes, Proceedings of the International Conference on Inner Shell Ionization Phenomena and Future Applications, April 17-22, 1972. CONF-720404, National Technical Information Service, U. S. Dept. of Commerce (1973) Vol. 1, p. 559.

15. C. J. Powell, Phys. Rev. Letters 30, 1179 (1973).

16. S. P. Kowalczyk, L. Ley, F. R. McFeely, R. A. Pollak, and D. A. Shirley, to be published.

17. A. Fahlman, R. Nordberg, C. Nordling, and K. Siegbahn, Z. Phys. 192, 476 (1966).

18. W. N. Asaad and E. H. S. Burhop, Proc. Phys. Soc. (London) 71, 369 (1958).

19. Kenneth D. Sevier, Low Energy Electron Spectroscopy (John Wiley and Sons, 1972). Reference is made to work by H. Hillig on sodium vapor Auger lines.

20. G. K. Wertheim, H. J. Guggenheim, and S. Hüfner, Phys. Rev. Letters 30, 1050 (1973).

21. T. Novakov, private communication.

22. C. J. Ballhausen, Introduction to Ligand Field Theory (McGraw-Hill, New York, 1962), p. 102.

Table I. Energies in the atomic copper ($L_3M_{45}M_{45}$; ^1D) Auger transition (in eV).

Quantity in Eq. (10)	Identity of This Quantity	Numerical Value	Reference
$E^A(j)$	$E(L_3)$	940.1	a,b
$E^A(k)$	$E(M_{45})$	10.44	b
$E^A(\ell)$	$E(M_{45})$	10.44	b
$\mathcal{F}(k,\ell;X)$	$\mathcal{F}(M_{45}M_{45};\ ^1D)$	25.9	b
$E_R(\ell)$	$E_R(3d)$	5.3	c

[a]The $\alpha_{12}\ L_{III}\ M_{IV,V}$ x-ray energy was taken from Ref. 11. The optical 3d energy was taken from Ref. 10.

[b]Ref. 10.

[c]This is termed the "reorganization energy" in Ref. 9.

Table II. Summary of results for the $(L_3M_{45}M_{45}; {}^1D)$ energy in copper.

Method	Est. Quantity	Value (eV)	R_e(expt)(eV)	R_e(theo)(eV)
E_B(solids)	$E^F({}^1D) - \mathcal{F}(M_{45},c)$	911.5	$\mathcal{F}(M_{45},c)$ = 6.5	11.0
E_B(atoms)	$E^A({}^1D)$	903.9	R_e(TA) = 9.6	15.5
E_B(atoms, 2-hole states)	$E^A({}^1D)$	902.4	R_e(TA) = 11.1	15.5

Table III. Values of parameters used in Eq. (16) to estimate $R_e(TA)_{expt}$ for the $(L_2M_{23}M_{23})$ transition (in eV).

Element	$E^A(L_3)$[a]	$E^A(3p)$[a]	$F^o(3p,3p)$[b]	$e\phi$[c]	E_R[d]	$E^F(L_3M_{23}M_{23})$[e]	$R_e(TA)_{expt}$[f]	$R_e(TA)_{theo}$[g]
K	300	24	17.1	2.2	(1.9)	248.9	8	11
Ca	357	34	19.3	(2.3)	(2.4)	288.6	12	17
Sc	410	39	20.9	3.5	(2.9)			29
Ti	467	45	22.5	4.3	3.4			31
V	525	51	24.0	4.3	(3.9)			32
Cr	584	83	25.2	4.5	(4.4)			36
Mn	653	63	27.0	4.1	(4.9)			38
Fe	722	70	28.4	4.5	5.3	596.7	28	41
Co	794	76	29.8	5.0	(5.8)	651.0	24	43
Ni	869	84	31.3	5.15	6.3	716.5	29	43
Cu	939	84	32.5	4.65	7.2	773.7	16	16
Zn	1028	98	34.1	3.7	(7.2)	832	16	14

[a] From Refs. 9 and 12.

[b] From Ref. 8.

[c] From Ref. 13, except K and Zn, from W. Gordy and W. J. O. Thomas, J. Chem. Phys. 24, 439 (1956); and Ca, estimated.

[d] From Ref. 9. Values in parentheses are interpolated.

(continued)

Table III. (continued)

[e] Ref. 14.

[f] From Eq. (17).

[g] Estimated as described in Ref. 6 and Sec. II.B. Screening orbitals were assumed to be 4s,p (K), 4p,3d (Ca), 4s,p (Cu), 4p (Zn), and 3d otherwise.

Table IV. Values of parameters used in Eq. (17) to estimate $R_e(TA)_{expt}$ for the $(L_3M_{45}M_{45})$ transition (in eV).

Element	$E^A(L_3) - E^A(3d)$[a]	$E^A(3d)$[b]	$F^o(3d,3d)$[c]	$e\phi$[d]	E_R[e]	$E^F(L_3M_{45}M_{45})$	$R_e(TA)_{expt}$	$R_e(TA)_{theo}$
Ti	452.2	8.3	17.0	4.3	2.0	452[f]	17	26
V	511.3	(9.5)	18.7	4.3	(2.5)	510[f]	17	28
Mn	637.4	10.8	21.9	4.1	3.6	637[h]	21	33
Fe	705.0	(11.6)	23.4	4.5	(3.9)	701.2[g]	19	37
Co	776.2	12.7	24.8	5.0	4.1	722.5[g]	22	39
Ni	851.5	(13.5)	26.3	5.15	(4.5)	848.0[g]	22	39
Cu	929.7	10.4	26.0	4.65	5.3	918.0[i]	10	15.5
Zn	1011.7	17.3	29.1	3.7	(5.3)	991.8[i]	12.4	17

[a] From $L\alpha_{12}$ x-ray energies, Ref. 11.

[b] From Refs. 9 and 12. Numbers in parentheses are based on interpolated reorganization energies. The Cu and Zn values are based on optical data (Ref. 10).

[c] From Ref. 8.

[d] As in Table III.

[e] From Ref. 9.

[f] T. W. Haas, J. T. Grant, and G. J. Dooley, Phys. Rev. B1, 1449 (1970).

[g] From Ref. 14.

[h] P. W. Palmberg, in Electron Spectroscopy, ed. by D. A. Shirley (North-Holland, 1972), p. 835.

[i] Ref. 6.

Table V. Parameters used in Eq. (18) to estimate R_e for the $M_5N_{45}N_{45}$ transition (in eV).

Element, Z	$E^F(M_5)$[a]	$E(N_{45})$[a]	$F^o(4d,4d)$[b]	E_R[c]	$E^F(M_5N_{45}N_{45})$	R_e
Ru, 44	281(1)	2.0(2)	15.3	7.7	280[d]	10.6
Rh, 45	307.5(10)	2.0(2)	16.3	8.2	306[d]	10.6
Pd, 46	335.4(10)	1.5(2)	16.3	9.0	328.6[a]	3.5
Ag, 47	368.5(3)	5.5(2)	18.1	10.6	351.7[a]	1.7

[a] This work. These energies were obtained by us in survey experiments, and do not represent the best accuracy obtainable.

[b] From Ref. 8.

[c] The reorganization energies from corresponding 3d elements were used, from Ref. 9.

[d] T. W. Haas, J. T. Grant, and G. J. Dooley, Phys. Rev. B1, 1449 (1970).

Table VI. Energy parameters for the Na(KLL; ^1D) Auger transition (in eV).

Sample	E(1s)[a]	E(2p)[a]	E(KLL; ^1D)[a]	R_e[d]	$\Delta[E(2p) - E_B(KLL)]$[e]
metal	1071.7	30.4	994.2	9.2	(8.7)
NaI	1070.3	28.3	991.9	4.1	4.3
oxide[b]	1075.2	32.8	986.8	3.1	3.7
NaF	(1066.8)[c]	24.8	991.9	(-0.2)	(0)

[a] Reference energies: top of valence bands (NaI and NaF); sodium Fermi level (metal and oxide).

[b] Thin oxide layer in metal.

[c] Estimated using E(1s) - E(2p) = 1042.0 eV.

[d] From Eq. (20).

[e] See Eq. (21). NaF was used as the reference.

Table VII. Energy parameters for the $Zn(L_3M_{45}M_{45};\ ^1D)$ Auger transition (in eV).

Sample	$E^F(2p_{3/2})$	$E^F(3d)$	$E^F(L_3M_{45}M_{45};\ ^1D)$	R_e [a]	$\Delta[E(3d) - E_B(^1D)]$
metal	1021.96[b]	10.18[b]	991.8[b]	6.8	5.2
ZnO	1022.2	10.44	987.4	2.7	1.0
ZnF_2	1021.5	10.9	985.9	2.8	(0)

[a] From Eq. (22).

[b] From Ref. 6.

FIGURE CAPTIONS

Fig. 1. (a) Difference between core-level binding energies for 3d-transition elements as atoms and metals, after Ref. 3, showing break between Ni and Cu due to reduction in extra-atomic relaxation energy on 3d-shell closure. (b) Total extra-atomic relaxation energy for the $L_3M_{23}M_{23}$ peak in these elements, with a localized final state. (c) Same for the $L_3M_{45}M_{45}$ transition, showing that the final state may be localized. In (a), (b), and (c) points represent experimental results while lines connect predictions of theory described in text.

Fig. 2. Sodium 1s, 2p, and ^1D Auger lines as observed in an XPS spectrum, plus free-atom energies. The 2p peaks are made to coincide. For the measured energies see Table VI. The 1s peaks nearly coincide, showing that the energy difference E(1s) - E(2p) is nearly constant, while large shifts arising from differences in extra-atomic relaxation are observed in the ^1D Auger lines. The free atom values are denoted by the arrows and bold lines. The lower binding energy component of the doublet in the Na 2p region in the NaF spectra is the F 2s peak.

Fig. 3. The $L_{2,3}M_{45}M_{45}$ Auger spectrum of ZnF_2.

Fig. 4. The Zn 3d - F 2p region of the XPS spectrum of ZnF_2.

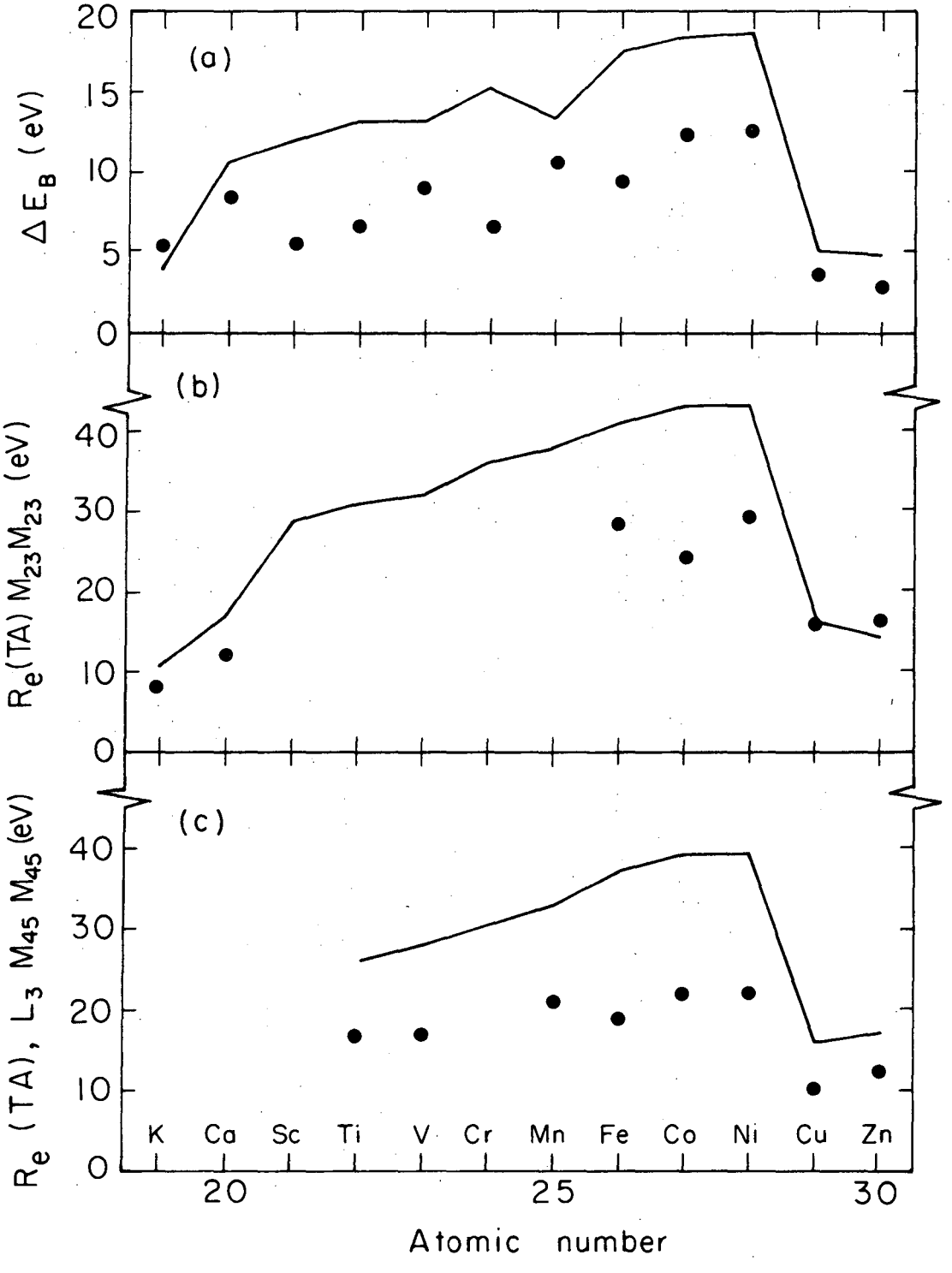
(a)
(b)
(c)
ΔE_B (eV)
$R_e(TA)\, M_{23}M_{23}$ (eV)
$R_e\,(TA),\, L_3\, M_{45}\, M_{45}$ (eV)
0
5
10
15
20
30
40
K
Ca
Sc
Ti
V
Cr
Mn
Fe
Co
Ni
Cu
Zn
20
25
30
Atomic number
XBL736-3136

Fig. 1

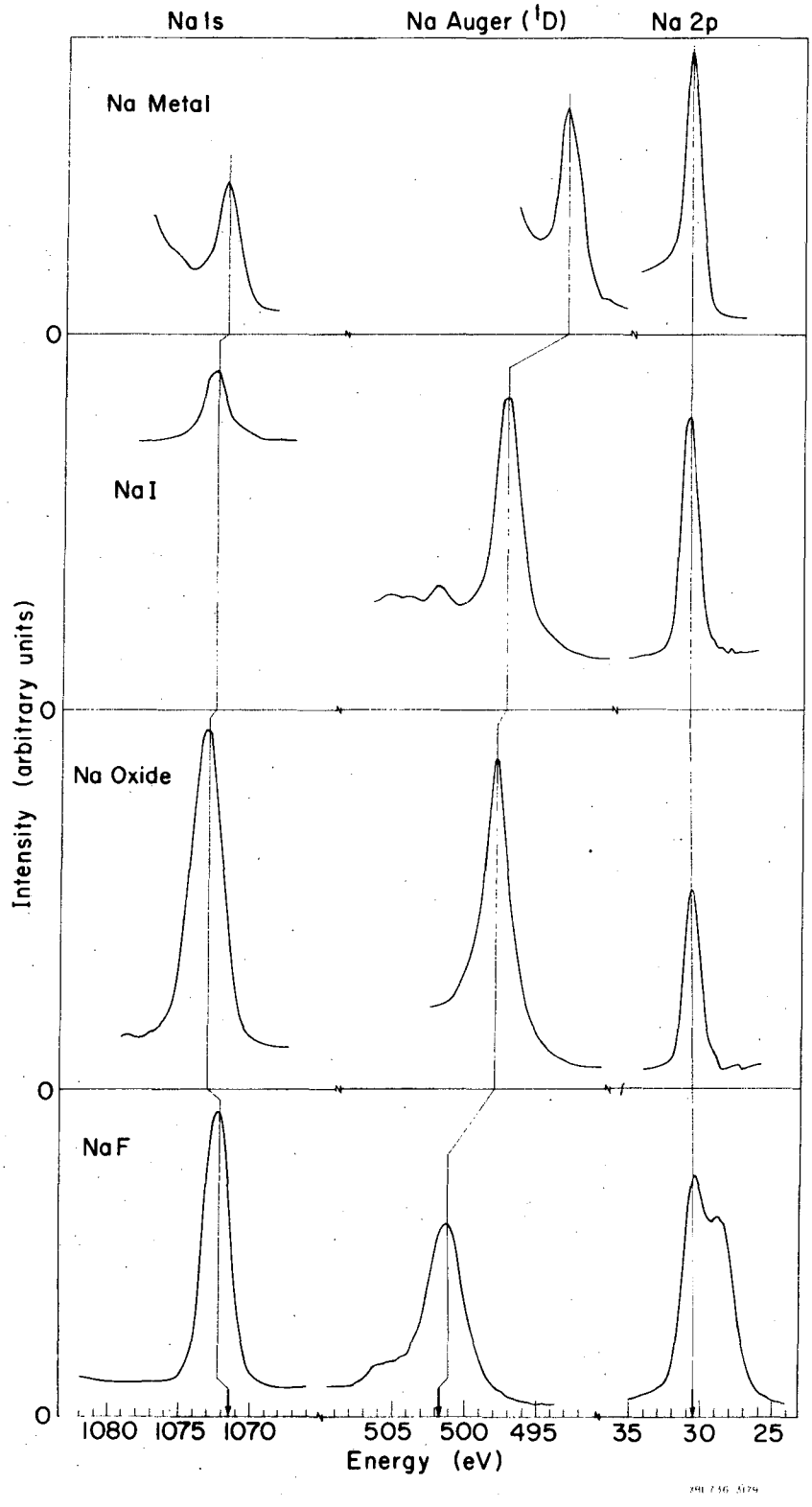
Na 1s
Na Auger (¹D)
Na 2p
Na Metal
NaI
Na Oxide
NaF
0
0
0
0
Intensity (arbitrary units)
1080 1075 1070
505 500 495
35 30 25
Energy (eV)

Fig. 2

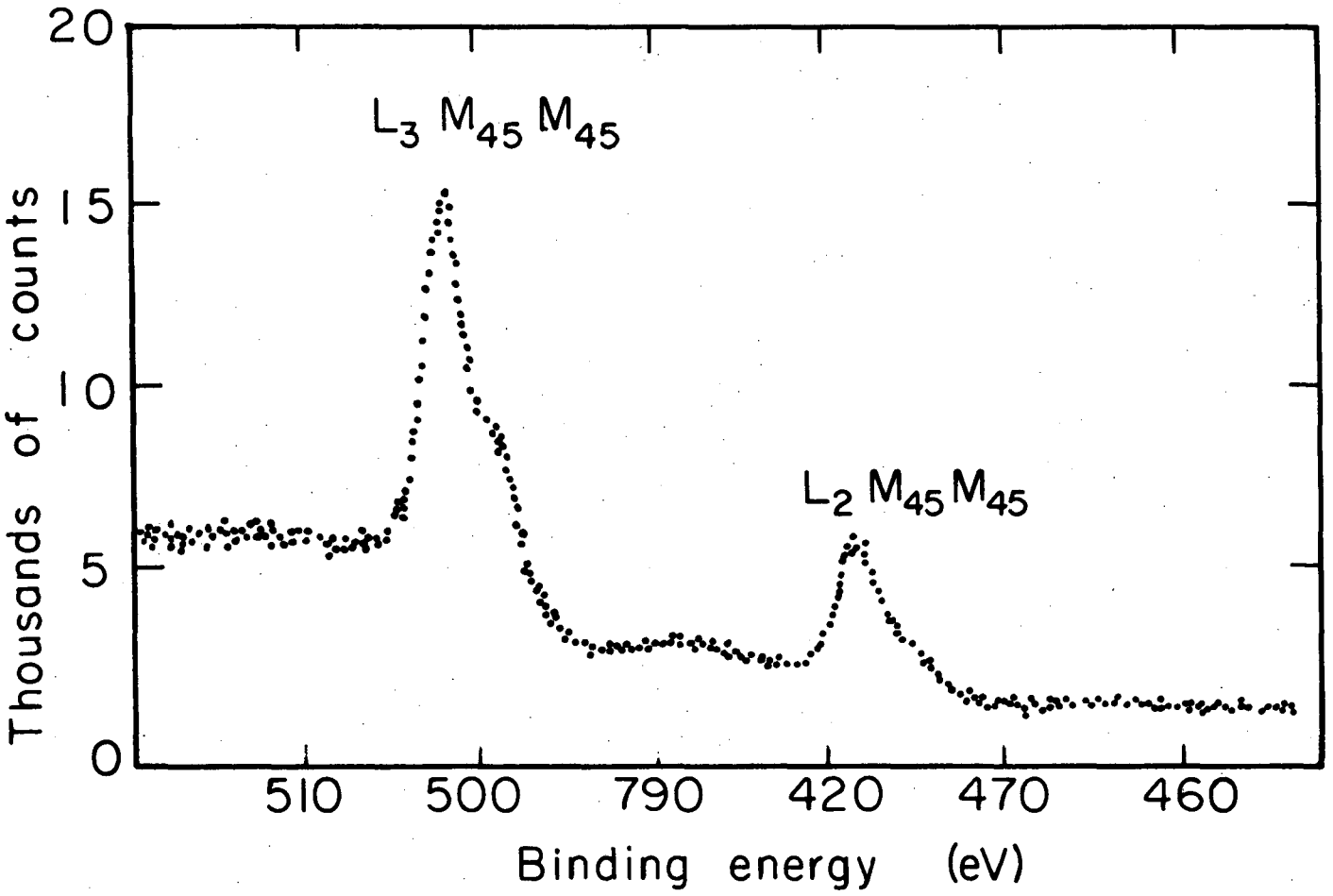

XBL736-3135

Fig. 3

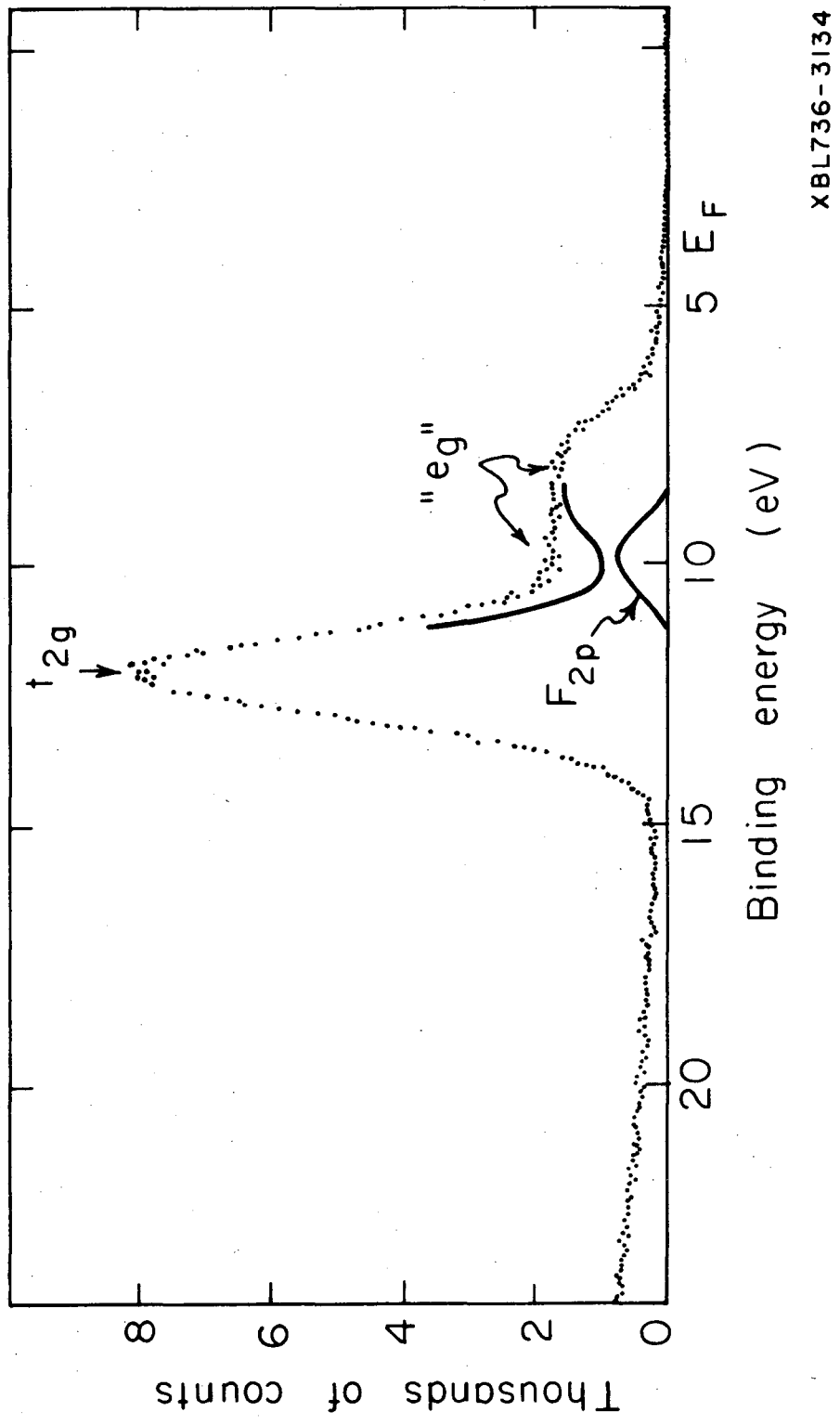
Thousands of counts
0
2
4
6
8
Binding energy (eV)
5
10
15
20
E_F
t_{2g}
"e_g"
F_{2p}
XBL736-3134

Fig. 4

TECHNICAL INFORMATION DIVISION
LAWRENCE BERKELEY LABORATORY
UNIVERSITY OF CALIFORNIA
BERKELEY, CALIFORNIA 94720